RSC Advances

PAPER

View Article Online
View Journal | View Issue

Cite this: *RSC Adv.*, 2014, **4**, 43912

How does PEDOT combine with PSS? Insights from structural studies†

Rupali Gangopadhyay,*[a] Bidisa Das*[a] and Mijanur Rahaman Molla[b]

Received 14th August 2014
Accepted 21st August 2014

DOI: 10.1039/c4ra08666j

www.rsc.org/advances

The severely intractable polymer poly(3,4-ethylenediethoxythiophene) (PEDOT) is brought to stable aqueous solution after *in situ* combination with polystyrene sulfonic acid (PSS). This solution (PEDOT–PSS) is stable and successfully combines the optical and electrical properties of PEDOT with the water solubility of PSS. This paper explores the physical properties of PEDOT–PSS from morphological and structural aspects and electronic structure studies are employed to understand the interaction between the two polymers. The solution consists of triangular/rectangular shaped nanoparticles and UV-vis spectroscopy is used to establish the highly doped and conductive nature of the sample with bipolarons present as carrier. Theoretical studies reveal the structure of the interpolymer complex and that the PEDOT chain is bent towards the PSS moiety, and thus, PEDOT–PSS is likely to form a partially coiled or helical structure. The unique stability of this system as well as its highly conductive nature is also consistent with the molecular model.

1. Introduction

Poly(ethylene-3,4-diethoxy thiophene) (PEDOT) stabilized in aqueous medium by poly(styrene sulfonic acid) (PSS) is an excellent material offering an optimum combination of the optical and electrical properties of PEDOT and the solubility of PSS. The severe intractability of PEDOT can be easily overcome by the formation of the interpolymer complex between PEDOT with PSS that makes a stable solution/dispersion in water (popularly known as PEDOT–PSS) which allows the polymer to be processed as a film/coating.[1,2] This solution/dispersion retains excellent redox coloration, moderate transparency, good electrical conductivity (1–10 S cm^{-1}) and many other important properties of PEDOT[3–6] and thus has wide application potential for various electronic devices. Bayer AG patented PEDOT–PSS a long time ago; their product is commonly known as Baytron®, of different grades. Agfa Materials, working with conductive polymer products (known as Orgacon™), have recently launched fifth generation formulations, including dry re-dispersible pellets of PEDOT–PSS.[7] Interestingly, this dispersion has unique stability on standing that has successfully been exploited commercially. This solution is extensively utilized worldwide in optoelectronic devices such as photovoltaic cells, light emitting diodes, electrochromic displays,[8–11] printing ink for inkjet printers,[12] and so on. However, the nature of the interaction between the two polymers and the underlying reason behind the solubilization of PEDOT after combination with PSS have remained almost unexplored.

Very recently, Fan *et al.*[13] and Dimitriev *et al.*[14] have tried to explore the structure and interaction of PEDOT–PSS by spectroscopic and morphological techniques. They have, however, focused their interest on improving the electrical conductivity of the material. The present work explores the nature of the interaction between PEDOT and PSS that ultimately leads to the unique stability of the dispersion. For the sake of good comparison, we have followed our own methodology to synthesize PEDOT–PSS solution in our laboratory, and we have studied its morphological and optical properties. Our experimental findings have been correlated with the theoretical studies of electronic structure and spectral properties to understand the nature of the interactions that are responsible for the unique properties of the doped polymer complex, for the first time. Although this system is not a solution in the proper sense, considering its unique stability in water, it will be termed as 'solution'.

2. Methodologies

2.1 Synthesis

3,4-Ethylenedioxythiophene (EDOT, monomer), PSS (M_w ~ 75 000) and $FeCl_3 \cdot 6H_2O$ were purchased from Sigma-Aldrich. In a typical synthesis, 90 mM stock solution of PSS was prepared in double distilled water. PSS solution (10 ml) was mixed with 60 μl of $FeCl_3$ solution (1.62 M), followed by addition of 20 μl of EDOT monomer with constant stirring. Several color changes were

[a]*Centre for Advanced Materials, India. E-mail: camrg@iacs.res.in; cambd@iacs.res.in*
[b]*Polymer Science Unit, Indian Association for the Cultivation of Science, 2A & 2B, Raja S C Mallik Road, Kolkata 32, India*

† Electronic supplementary information (ESI) available: Details of the experimental part and theoretical modeling of EDOT trimers and octamers, and a few SEM pictures are available free of cost at http://www.rsc.org. See DOI: 10.1039/c4ra08666j

observed and finally a dark blue PEDOT–PSS solution was synthesized. The product was further purified by dialysis[4] with deionised water for three consecutive days and the water was changed every day. The dialysis membrane, which was purchased from Membrane Filtration Products (M_w cut off = 3500), could remove the ions, low molecular weight oligomers and unreacted monomer from the solution. However, the excess PSS and Fe^{3+} ions complexed to the PSS structure could not be removed, as was observed from further experiments. The same technique was followed for synthesis of a set of three PEDOT–PSS solutions (P-1, P-2, P-3) by varying the amount of monomer (15 μl, 20 μl and 25 μl); P-2 was considered to have the optimum composition.

2.2 Transmission electron spectroscopy (TEM)

The stable PEDOT–PSS solution was diluted 20-fold with water, and no precipitation was observed. One drop of the optically clear dispersion was taken on to the TEM grid and analysed at 200 kV using a JEOL JEM-2010 electron microscope.

2.3 Scanning electron spectroscopy (SEM)

Morphological studies of the sample were done using a JEOL JSM-6700F scanning electron microscope at 200 kV.

2.4 Dynamic light scattering (DLS)

A diluted PEDOT–PSS solution, as used for SEM, was subjected to DLS studies using a Brookhaven Instruments BI-200SM goniometer.

2.5 UV-Visible absorption spectroscopy (UV-vis)

The as-prepared PEDOT–PSS solution was diluted with water and subjected to UV-vis spectroscopic measurements using a Shimadzu UV-2550 spectrophotometer. Respective UV-vis spectra were recorded by changing the pH from 2 (original) to 1 (HCl), 5 (NH_4OH) and 10 (NaOH).

2.6 Electrical conductivity

Spin coated and dried film of the solutions were subjected to conductivity measurement using a four-probe measurement technique.

2.7 Theoretical studies

The electronic structure studies for the doped and undoped EDOT oligomers were performed using density functional theory (DFT) as implemented in the Gaussian 03[15] suite of programs. Studies of oligomeric EDOT, styrene sulfonic acid (SS) and EDOT–SS complexes were performed using the B3LYP[16,17] hybrid functional with the 6-31G** basis sets for all atoms. The stable structures of all isolated molecules and complexes were determined by full geometry optimization in the gas phase and consequent harmonic frequency calculations were performed to ascertain the stationary points. The frontier molecular orbitals, especially the highest occupied molecular orbital (HOMO) and the lowest unoccupied molecular orbital (LUMO) of free PEDOT and PSS and the complex (PEDOT–PSS), were analyzed. The charge distribution was determined using Mulliken's method for all the systems studied. To simulate the UV-vis spectra of the polymeric systems, transition energies and oscillator strengths for electronic excitation to the first 50 singlet excited states of various PEDOT oligomers (complexed and uncomplexed) were calculated using time dependent density functional theory (TD-DFT) using B3LYP/6-31++G** methodology. However, because TD-DFT studies are highly resource consuming we carried out calculations where only the oligomeric PEDOT cation was considered to be fixed in the geometry of the PEDOT–PSS complex. This was not unreasonable because the UV-vis spectra of these systems are experimentally found to be unaffected by the anionic moiety. The UV-vis spectra were plotted using GaussView software (Scientific Software Solutions). We also determined all the transitions and identified the molecular orbitals involved using the application software SWizard.[18]

3. Results and discussion

The schematic presentation of the PEDOT–PSS interpolymer complex is shown in Scheme 1. It is obvious that PSS, in this assembly, serves not only as a dispersant of PEDOT but also as a charge compensating counter-polyanion to the PEDOT backbone yielding a primary PEDOT–PSS structure at the molecular level. The secondary as well as the tertiary structure of this complex consists of charged EDOT oligomers (~6–18 repeating units) distributed along a high molecular weight PSS chain, as proposed by Dimitriev *et al.*[14]

3.1 Morphology (TEM and DLS)

We observed PEDOT–PSS particles of a very similar size and shape from the three sets of solutions using the TEM and SEM images, as shown in Fig. 1a and b. Therefore, it can be stated that the particle size and morphology of PEDOT–PSS is independent of the initial concentration of monomer. Unlike spherical particles, which are generally obtained in dispersed systems, PEDOT–PSS consists of rectangular and triangular

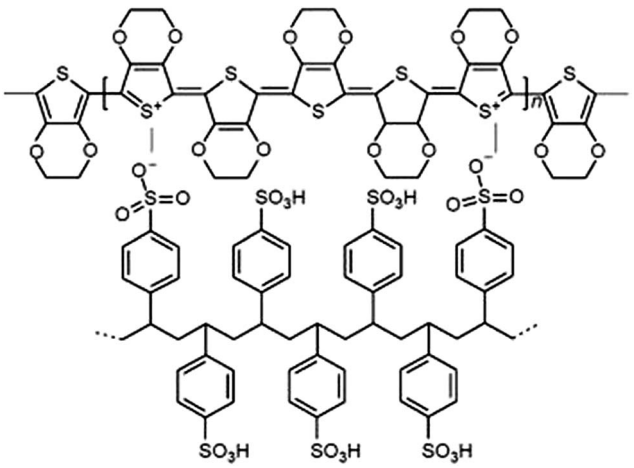

Scheme 1 The possible combination between PEDOT and PSS.

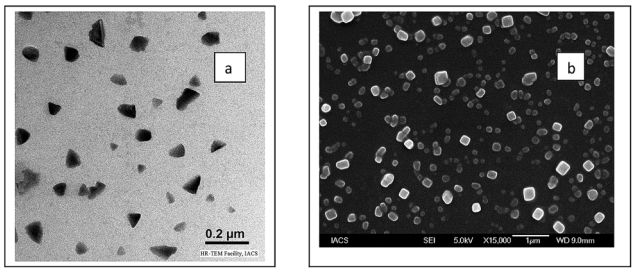

Fig. 1 Particle size and morphology of PEDOT–PSS solution as obtained from (a) TEM & (b) SEM.

shaped discrete particles with two different size ranges, as observed from the TEM and SEM images. In the as-prepared samples (diluted thoroughly), particles of two different size ranges, namely, ~70–100 nm and ~400 nm were frequently observed. The sharp contrast of the particles indicates the large $\prod$ electron density commonly obtained for conjugated conducting polymers. In the DLS studies of the as-prepared samples, particles having diameter in the range of 20–25 nm, 70–85 nm and 650–970 nm were initially identified (Fig. 2a). When the study was repeated with thoroughly sonicated samples, the association among the particles was destroyed and particles of two size ranges, 25–35 nm and 350–460 nm, were obtained in the DLS spectrum (Fig. 2b) whereas larger structures disappeared from the SEM image (Fig. S1†).

Therefore, it can be stated that freshly prepared PEDOT–PSS particles are smaller in size and dispersed in the medium. However, as a result of the multivalent Fe^{3+} the outer PSS^{-} layer undergoes some degree of association that gives rise to the larger particles. Dimitriev *et al.*[14] previously explored this system and showed the possibility of three types of interaction (primary, secondary and tertiary) within the system. They also showed small PEDOT particles distributed along the PSS chain (secondary structure) and larger gel-like particles consisting of a coiled PEDOT–PSS chain. However, from the TEM and SEM images and DLS spectra, it can be inferred that, despite complete dissociation of PSS in water, the PEDOT–PSS complex does not stay in a molecular wire/nanotube-like open structure, but rather remains in a partially coiled form as explained earlier.[13] Our electronic structure studies on this system also corroborate the formation of a coiled structure.

3.2 UV-vis spectroscopy

As PSS has no absorption above 310 nm, the spectral response of PEDOT–PSS comes from the PEDOT moiety. The absorption spectra of three sets of PEDOT–PSS solutions (pH 2) more or less retain the spectral properties of PEDOT (Fig. 3a). The higher energy peak at ~340 nm is assigned to the n–Π* transition in the PEDOT backbone and the broad band above 800 nm corresponds to bipolaron subgap states[19–21] indicating the heavily doped and conductive nature of the sample.

On increasing the concentration of PEDOT, no spectral shift was observed but the absorption intensity increased over the whole range. Therefore, in the present system, PEDOT–PSS interaction is independent of PEDOT concentration. UV-vis spectra were also recorded on changing the pH from 2 (original) to 1 (HCl), 5 and 10 (NaOH). On increasing the pH (adding NaOH) to 5 and 10, PSS anions are removed from the PEDOT–PSS assembly, which destroys the mutual interaction between the polymers and breaks down the three-dimensional structure of the system. This conformational change hampers the carrier transport in the system, as a result of which the bipolaron band in the near-infrared (NIR) region flattens. On lowering the pH, the effect is reversed and the PEDOT–PSS interaction becomes stronger because of conformational effects. As a result, carrier transport is favored (although the doping level is unaltered) and the band at ~800 nm becomes prominent (Fig. 3b). Yamashita *et al.*[22] have also previously reported a similar effect of pH on the conductivity of PEDOT–PSS, whereas some other groups have observed improvement of conductivity in the presence of inert solvents such as sorbitol and polyethylene glycol and have termed this effect as secondary doping.[13,23] Our samples have shown electrical conductivity of the order of 10^{-1} S cm^{-1} (*P*2: 0.6 S cm^{-1}), which is a moderately high value, similar to that obtained earlier.[13,22,23] Dimitriev *et al.*[14] have made some attempt to enhance the conductivity of the system by controlling the interaction between PEDOT and PSS and have probed it spectroscopically. We have followed quantum mechanical

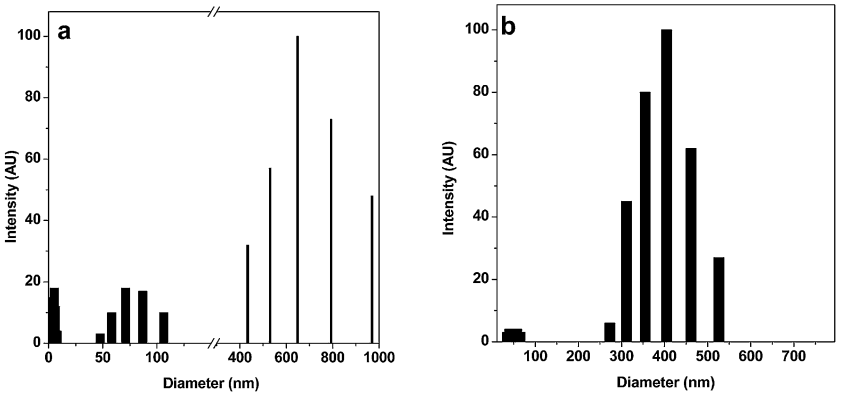

Fig. 2 DLS spectra of PEDOT–PSS solution showing the particle size distribution in the system (a) before sonication, (b) after sonication.

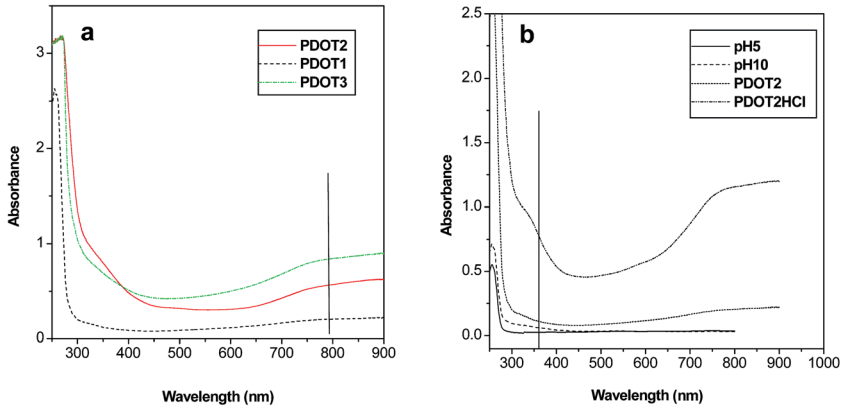

Fig. 3 UV-vis absorption spectra of PEDOT–PSS solutions at (a) different concentrations and at (b) different pH values.

calculations (to be discussed later) that have also revealed the appreciably high conductive nature of the system. Therefore, the experimental part of our work has established PEDOT–PSS to be a highly doped, electrically conductive system with good solution stability but of an entangled and polydispersive nature.

3.3 Quantum mechanical studies

3.3.1 Structural studies. Several theoretical studies have been published for oligomeric, undoped polythiophenes[24–27] but those for PEDOT and PSS are scarce. In two studies, the interaction between single units of SS/toluene sulfonate with small oligomeric units of EDOT were considered.[28,29] These studies are somewhat unrealistic, because mutual interactions between two monomeric units does not necessarily represent the interactions in the large polymeric systems. In the present work structural and electronic properties of the PEDOT–PSS interpolymer complex in oligomeric forms have been studied from three aspects. (1) The geometry of the polymeric assembly was optimized initially, which is indeed one of the primary objectives of this study. (2) The description of the charge distribution on the conjugated polymeric chain is crucial, because the electrostatic interactions are expected to play a major role in determining the supramolecular arrangement and thus, we report the electronic charge distribution (Mulliken type) of the EDOT oligomer and its complex with the SS oligomer in the next step. (3) The energy gap between HOMO and the LUMO is an important factor, which gives an indication of the ease with which their electron densities can be modified. This is an essential criterion for conducting molecules and we have reported this for PEDOT and PSS and the complex (PEDOT–PSS), in doped and undoped forms. To make the large polymeric systems tractable and to minimize the computational resources used, we have used oligomers of EDOT and SS, instead of long chain polymers (Scheme 1). To clearly understand the interactions present in EDOT oligomers doped with SS anions, we have modeled the PEDOT as oligomers of three (3-mer EDOT) and eight (8-mer EDOT) units and SS as dimer and tetramer. Monocation ($EDOT^{+}$) and dication ($EDOT^{2+}$) for the trimer, and dication ($EDOT^{2+}$) and tetracation ($EDOT^{4+}$) for the 8-mer were studied theoretically, which is in line with the formation of polaronic charge carriers. The studies of the trimer, monocations and dications and their respective complexes with SS anions are included in the ESI (Fig. S2–S4†). We have chosen to further reduce the size of the PEDOT 8-mer by removing the ethylene oxide rings connected to the two edge thiophene units. This slight modification of structure does not affect the molecular orbitals or charge distribution of the EDOT unit as we have shown in the ESI (Fig. S5 and S6†). It has earlier been pointed out that[24] for oligothiophenes longer than six units, the energy of the unrestricted wave function is lower than the energy of the restricted wave function. This indicates that the dications of very short oligomers are stable in the bipolaronic state, however, for dications of longer oligomers, the polaron pair configuration (two separated cation radicals) contributes significantly to the ground-state structure. To ascertain the stability of the singlet state for the EDOT oligomers, we have studied the dication of EDOT 8-mer as a singlet (both restricted RB3LYP and unrestricted UB3LYP) and open-shell, unrestricted triplet species and we found that the singlet, restricted state is slightly more stable (4.3 kcal mol^{-1}) than the unrestricted triplet state.

The relaxed structures of EDOT, $EDOT^{2+}$ and $EDOT^{4+}$ 8-mers are all planar and the tetracationic form is shown in Fig. 4a together with the relaxed structures of SS^{2-}/SS^{4-} (Fig. 4b and c). It is observed that, if the SS^{2-}/SS^{4-} unit is placed above the EDOT chain, it no longer remains planar and is bent concave to maximize the interaction with the anion (Fig. 4d and e). This, however, indicates that PEDOT and PSS do not stay parallel to each other to form a molecular wire/tube-like structure; rather, with an increase in chain length and charge density, the chain is gradually entangled/coiled as shown by the TEM/SEM images. This is in contrast to the study[30] reported by Dkhissi *et al.* where the authors carried out theoretical studies of the structure of doped PEDOT using a combination of *ab initio* and molecular mechanics methods in the presence of PSS counterions. They, however, froze the structure of PEDOT to a planar conformation, which did not allow them to check the deformation in the cationic backbone of the complex.

3.3.2 Charge distribution. For PEDOT 8-mer we studied the neutral, dicationic and tetracationic species, in singlet states.

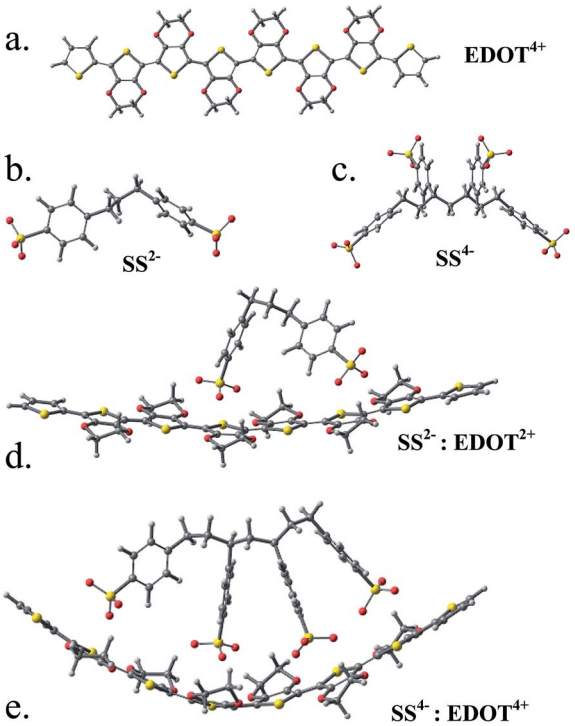

Fig. 4 Optimized structures of (a) eight units of EDOT (tetracationic state), (b) two units of SS (dianionic state), phenyl groups are far from each other. (c) Four units of SS (tetraanionic state), phenyl groups move away from each other. (d) Complex formation between dicationic EDOT and dianionic SS ($EDOT^{2+}$–SS^{2-}), which as a whole is neutral. (e) Complex formation between tetracationic EDOT and tetraanionic SS ($EDOT^{4+}$–SS^{4-}), which is neutral as a whole.

The nature of bond alternation for the uncomplexed EDOT, $EDOT^{2+}$ and $EDOT^{4+}$ is shown in Fig. 5a. The double bonds (1.38–1.39 Å for C=C) are shown in a red color and it is clear that undoped EDOT is largely aromatic, while the dication has contributions from quinonoid structures. The bond lengths of the tetracation are partially quinone-like. In the doped dicationic complex $PEDOT^{2+}$–PSS^{2}, the charged sulfonate groups interact with the $PEDOT^{2+}$ chain and the closest distances of the O-atoms of the two sulfonate groups to the thiophene S atoms are 3.2 Å and 3.5 Å. The binding energy of the SS^{2-} to $EDOT^{2+}$ is found to be reasonably large (183.85 kcal mol^{-1}, details in ESI†). Interaction between $EDOT^{4+}$–SS^{4-} is stronger compared to $EDOT^{2+}$–SS^{2-} where each of the four sulfonate groups interacts with thiophene moieties and a binding energy as large as 629.8 kcal mol^{-1} is observed. As expected, the structure shows a close positioning of the negatively charged sulfonate groups on top of the EDOT chain where the positive charges are accumulated and the closest distance of approach of the O atoms of the $–SO_3H$ group to the thiophene S are 3.2–3.6 Å.

The Mulliken atomic charges for the uncomplexed EDOT, $EDOT^{2+}$, $EDOT^{4+}$, $EDOT^{2+}$–SS^{2-} and $EDOT^{4+}$–SS^{4-} are shown in Fig. 5b–e. The charge distribution of uncharged EDOT (Fig. 5b) shows that, for the singlet optimized geometry, there are negligible charges on the central rings of the backbone compared with the other rings, with the charge slightly increasing from the middle and then decreasing drastically for the two end rings. This finding matches with the study of the uncharged neutral trimer which is included in the ESI.† The same trend is observed for $EDOT^{2+}$ although the charges are significantly higher in this case. For example, in $EDOT^{2+}$ (Fig. 5c), the atomic charges are 0.20, 0.26, 0.27, 0.27, 0.27, 0.27, 0.26, and 0.20 for the eight thiophene rings. Indeed, according to Fig. 6a, the end rings are aromatic, whereas the other rings are quinoid. This phenomenon of increasing charge from the middle to the ends of the chain is especially pronounced for the tetracation $EDOT^{4+}$ (Fig. 5d). $EDOT^{4+}$ has atomic charge distribution of 0.54, 0.49, 0.49, 0.43, 0.43, 0.49, 0.49 and 0.54 for the eight rings. This pattern represents the presence of two separated polarons at the two sides of the chain, with the separation region lying in the middle of the chain. The charges calculated on the rings after complexation of $EDOT^{2+}$ with monomeric SS^{2-} are positive and are 0.04, 0.11, 0.24, 0.25, 0.31, 0.39, 0.25 and 0.07 on the eight rings (Fig. 5e). Since the anion is not positioned exactly on top of the centre of the molecule, the charge distribution is not symmetrical and the maximum positive charge is on the rings which directly face the $–SO_3H$ groups of the anion, indicating a strong interaction and a possibility of a helical/coiled structure of the complex. When $EDOT^{4+}$ interacts with the styrene sulfonate tetramer, SS^{4-}, there is still more bending of the cationic EDOT (see Fig. 4), and the average charges on the rings after complexation are calculated as 0.20, 0.44, 0.37, 0.42, 0.38, 0.48, 0.49 and 0.21. The thiophene rings, which face the sulfonate groups show more pronounced charges and because the anion is not placed symmetrically the overall symmetry in the charge distribution is also lost after complexation.

3.3.3 Molecular orbitals. The molecular orbitals of all the systems studied are shown in Fig. 6. For EDOT, the HOMO and LUMO are shown in Fig. 6a, which shows extended conjugation of pi orbitals over the entire length of the molecule as is expected for aromatic systems. The HOMO–LUMO energy gap is calculated to be 2.25 eV. For the $EDOT^{2+}$–SS^{2-} complex, the HOMO–LUMO energy gap decreases to 1.09 eV and for $EDOT^{4+}$–SS^{4-} it further decreases to 0.74 eV. A systematic decrease of the HOMO–LUMO gap definitely indicates that the electronic density of the system could be more easily modified, and thus, electrical conductivity for the doped systems are high, as obtained experimentally. For the $EDOT^{2+}$–SS^{2-} complex the HOMO is mainly localized on the EDOT portion with slight contributions from the $–SO_3H$ groups of the anion, whereas the HOMO − 1 orbital is mainly localized on the anionic portion. LUMO and LUMO + 1 are primarily localized on the EDOT portion (Fig. 6b).‡ For $EDOT^{4+}$–SS^{4-}, HOMO and HOMO − 1 are localized primarily on the EDOT portion, whereas the unoccupied LUMO and LUMO + 1 are primarily localized on the SS^{4-} (Fig. 6c). From UV-vis spectra we have identified PEDOT–PSS as a highly conductive system with a large carrier tail at the NIR region. Simulation also identified separated polarons on the PEDOT backbone. However, in heavily doped systems such as

‡ HOMO − n is the nth MO lower in energy than HOMO and LUMO + n is the nth MO higher in energy than the LUMO.

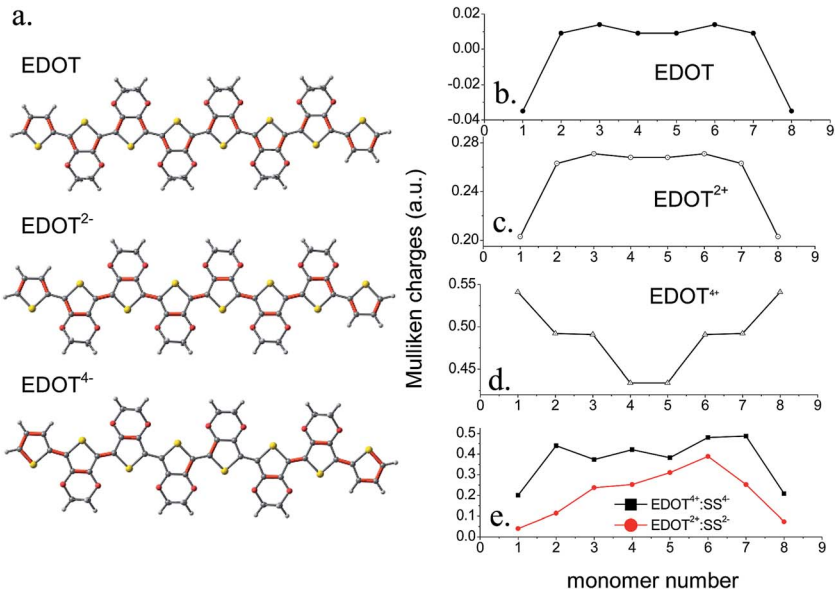

Fig. 5 (a) Nature of bond alternation in EDOT, $EDOT^{2+}$ and $EDOT^{4+}$. The red bonds are aromatic double bonds (1.38–1.39 Å for C=C and 1.70 Å for C=S). (b) Mulliken charges for EDOT. (c) Mulliken charges for $EDOT^{2+}$. (d) Mulliken charges for $EDOT^{4+}$. (e) Mulliken charges for $EDOT^{2+}$–SS^{2-} and $EDOT^{4+}$–SS^{4-}.

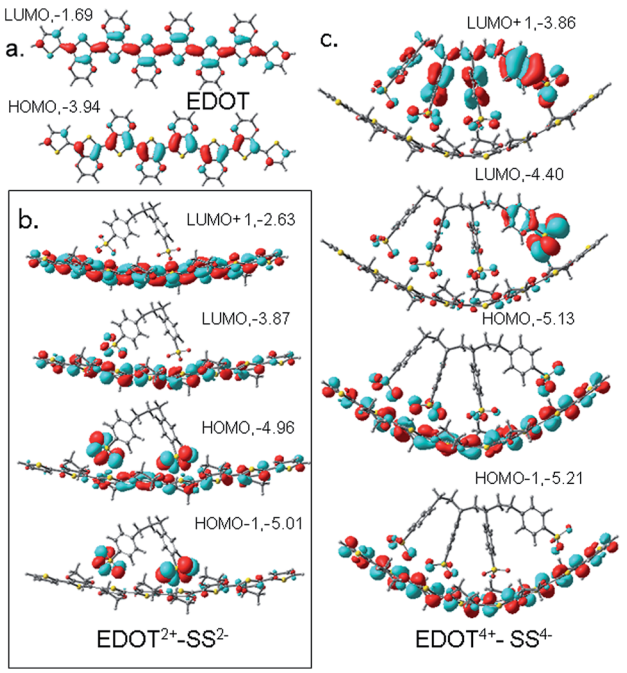

Fig. 6 (a) Nature of HOMO and LUMO in EDOT; (b) nature of HOMO − 1, HOMO, LUMO and LUMO + 1 in $EDOT^{2+}$–SS^{2-}; (c) nature of HOMO − 1, HOMO, LUMO and LUMO + 1 in $EDOT^{4+}$–SS^{4}. The red and cyan colors represent different signs of the wave functions in the molecular orbitals. The energies of the orbitals are reported in eV.

PEDOT–PSS, bipolarons are most likely to be present as carriers as established earlier.[20–23] At this point the experimental results do not match with the theoretical observations, but it should be remembered that the theoretical studies are performed on very small chains (8-mer) and without any solvent effects, therefore, we cannot expect all the theoretical results to perfectly match the experimental results. However, that there is intimate interaction between two polymers that ultimately leads to a uniquely stable envelope such as the structure of PSS on PEDOT is established from theoretical studies together with the detailed geometries and charge distributions. This conclusion was indirectly drawn earlier from different studies but was not established theoretically.

3.3.4 UV-vis spectra. The UV-vis spectra allowed comparison of the results of theoretical studies with reality (experiment). We constructed the UV-vis spectra of $PEDOT^{2+}$ (dication), $PEDOT^{2+}$–PSS^{2-} (dication–dianion) and $PEDOT^{4+}$–PSS^{4-} (tetracation–tetraanion) using TD-DFT methodology (Fig. 7). The qualitative difference between these three spectra should reflect the effect of cation–anion interaction and the related bending of the polymeric complex, as already observed from Fig. 4. It should be remembered that the results are only qualitatively comparable because, unlike highly conjugated, high molecular weight PEDOT–PSS, the theoretical models are limited to only 8-mers. Additionally, the solvent effect was not included in the theoretical modeling, which might also cause some deviation from the experimental spectra. However, the electronic transitions in the original polymer and their changes in the PEDOT–PSS complex are largely comparable.

Analysis of the electronic transitions calculated using TD-DFT reveals that the most intense transition in these samples is at ~900 nm with an oscillator strength >3 which corresponds to the HOMO to LUMO transition in the polymer. For planar $PEDOT^{2+}$ without PSS^{2-} (Fig. 7a), two intense peaks appear at ~300 nm and ~415 nm because of transitions from HOMO to LUMO + 2, HOMO − 1 to LUMO + 1 and HOMO − 4 to LUMO + 2 orbitals. These peaks are almost retained in the dicationic

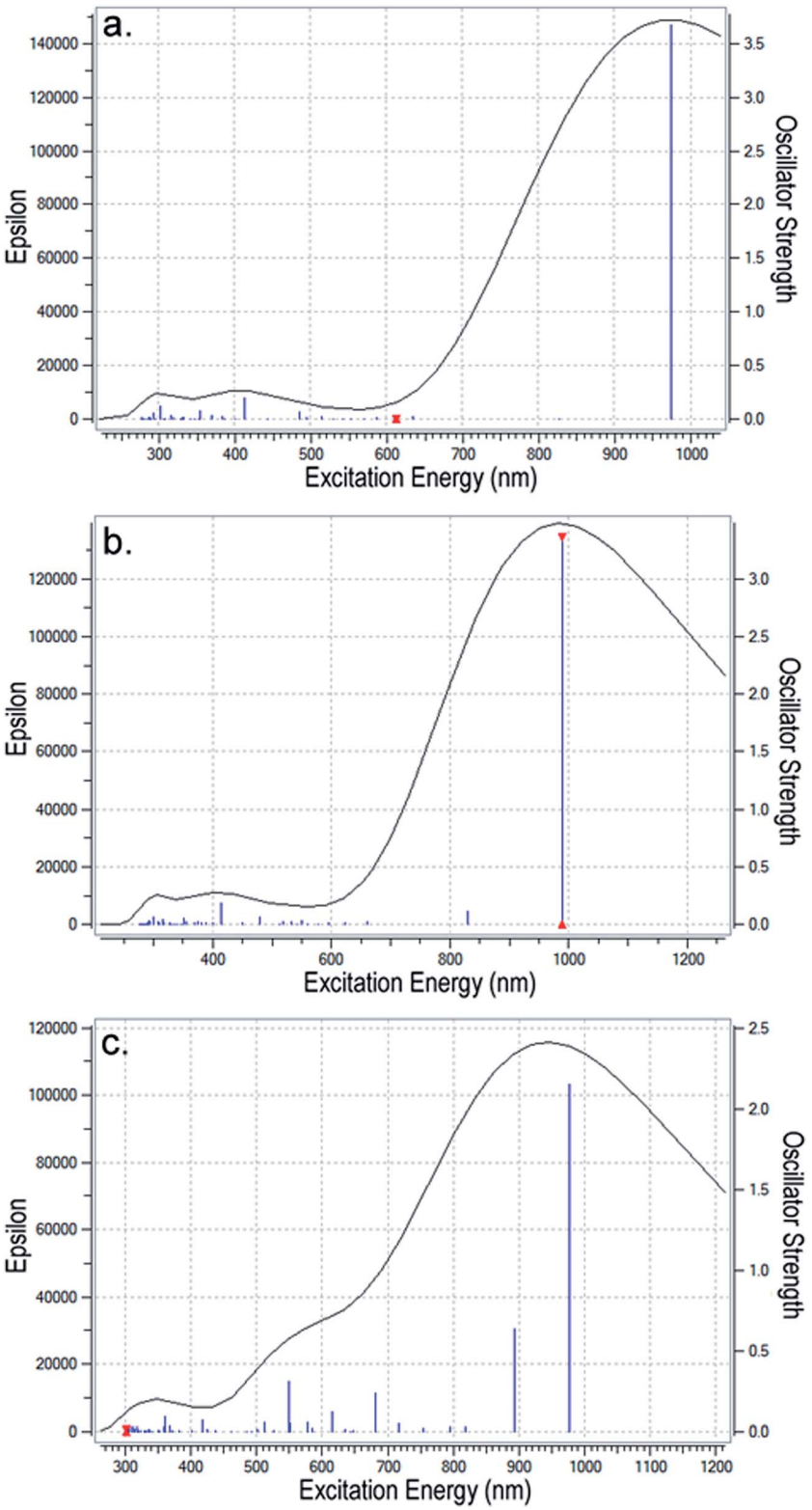

Fig. 7 The UV-vis spectra for (a) $PEDOT^{2+}$ (without PSS^{2-} counterion); (b) $PEDOT^{2+}$ slightly bent to interact with the dianion; and (c) $PEDOT^{4+}$ with more bending when it interacts with the tetracation.

complex (Fig. 7b) but are shifted and overlapped with other weak transitions from inner occupied orbitals to LUMO or LUMO + 1/LUMO + 2 orbitals to create a hump in the 300–400 nm region in the bent tetracationic complex. At the same time, several transitions from inner occupied states to the LUMO + 1 orbital takes place in the curved dicationic and bent

tetracationic complexes that appear in the region of 550–650 nm. As a result, the valley in the 500–600 nm region gradually diminishes and a broader hump above 500 nm appears for the tetracationic sample (Fig. 7c). Enlarged versions of these figures are included in the ESI (Fig. S7(a)–(c)†). As we compare the results of the theoretical spectra with our own experimental results (Fig. 3a and b) and also those from earlier investigations, we observe good agreement. The bands at lower wavelengths (370 nm, 415 nm) are assigned to the n–$\prod$* transition in the polymer and the broad hump above 900 nm is assigned to the bipolaronic transition.[19–21] The large bipolaronic hump indicates the highly conductive nature of the samples. Furthermore, the gradual broadening of the bipolaronic hump in the polymeric complex is also accounted for by macroionic interactions and related bending of the total moiety. As the polymeric complex is bent gradually, degeneracies of different energy levels are disturbed and several weaker transitions take place within the 500–600 nm region, which result in the observed broadening of the bipolaronic peak. Earlier studies have also experimentally established similar changes in UV-vis spectra with an increase in the extent of cation–anion interaction in the PEDOT–PSS system.[14,31] The theoretical modeling of the UV-vis spectra helps us to understand the origin of the electronic transitions and subsequent changes occurring upon interaction with the counterion. This helps to resolve the nature of interaction between the components and supports the formation of a bent/helical polymeric structure.

To summarize, the theoretical studies indicate that: (1) PEDOT and PSS oligomers do not stay parallel to each other to form a molecular wire tube-like structure after polymerization – rather, with increase in chain length, the chain is gradually bent around the anionic PSS unit; (2) atomic charge distribution patterns in the PEDOT–PSS oligomers represent the presence of two separated polarons at the two sides of the chain, and the asymmetry in charge distribution also suggests coiled/helical complex formation; (3) analysis of molecular orbitals and HOMO–LUMO gaps indicates a strong conducting nature; and (4) the simulated optical spectra are very similar to experimentally obtained spectra and support the conducting nature.

4. Conclusion

This article explores the nature of interaction between the two polymers PEDOT and PSS which combine to form a well-known aqueous solution with many unique properties. From experimental and theoretical studies we have observed that, unlike other dispersed systems, PEDOT particles are not dispersed in the PSS matrix; rather, PEDOT–PSS particles as a whole are enveloped in an outer PSS–water medium that is the key reason for the unique stability of this solution. PEDOT and PSS form a supramolecular assembly of unique stability in aqueous medium; even oligomers such as 8-mer/3-mer of PEDOT, which are fully planar in isolated form, gradually bend to maximize the interactions with the counterion with thiophene rings facing the sulfonate groups. This indicates the possibility of the formation of a partially coiled or helical structure of the interpolymer complex leading to the formation of particles in reality (as found in the TEM and SEM images) rather than simple side-by-side interaction leading to molecular wires. The helical structure as well as the highly conductive nature of the sample were also supported by the models of UV-vis spectra of the polymeric complex. It is hoped that this understanding will pave the way for new studies with PEDOT that will lead to new insights and more control over the physical and optical properties of PEDOT.

Acknowledgements

Corresponding authors acknowledge SERC-DST (India) for financial assistance, project no. SR/FT/CS-119/2010 & SR/WOS-A/CS-77/2011. MRM acknowledges CSIR (India) for granting an SRF.

References

1 A. G. Bayer, Eur. Patent 440957, 1991; A. Gevaert, Eur. Patent 564911, 1993.
2 S. Kirchmeyer and K. Reuter, *J. Mater. Chem.*, 2005, **15**, 2077.
3 L. Groenendaal, F. Jonas, D. Freitag, H. Pielartzik and J. R. Reynolds, *Adv. Mater.*, 2000, **12**, 481.
4 H.-E. Yin, F.-H. Huang and W.-Y. Chin, *J. Mater. Chem.*, 2012, **22**, 14042.
5 R. W. Heuer, R. Wehermann and S. Kirchmeyer, *Adv. Funct. Mater.*, 2002, **12**, 89.
6 A. N. Aleshin, S. R. Williams and A. J. Heeger, *Synth. Met.*, 1998, **94**, 173.
7 http://www.conductive-polymer.com/orgacon-conductive-inks.html.
8 F. Jonas, W. Craft and B. Muys, *Macromol. Symp.*, 1995, **100**, 169.
9 M.-A. De Paoli, G. Casalbore-Miceli, E. M. Girotto and W. A. Gazotti, *Electrochim. Acta*, 1999, **44**, 2983.
10 Y. Cao, G. Yu, C. Zhang, R. Menon and A. J. Heeger, *Synth. Met.*, 1997, **87**, 171.
11 J. Ouyang, C.-W. Chu, F.-C. Chen, Q. Xu and Y. Yang, *Adv. Funct. Mater.*, 2005, **15**, 203.
12 Y. Yoshika and G. E. Jabbour, *Synth. Met.*, 2006, **156**, 779.
13 B. Fan, X. Mei, J. Ouyang, B. Fan, X. Mei and J. Ouyang, *Macromolecules*, 2008, **41**, 5971.
14 O. P. Dimitriev, Y. P. Piryatinski and A. A. Pud, *J. Phys. Chem. B*, 2011, **115**, 1357.
15 M. J. Frisch, *et al.*, *Gaussian 03, Revision C.02*, Wallingford-CT, 2004.
16 A. D. Becke, *J. Chem. Phys.*, 1993, **98**, 5648.
17 A. D. Becke, *Phys. Rev. A*, 1998, **38**, 3098.
18 S. I. Gorelsky, *SWizard program*, University of Ottawa, Ottawa, Canada, 2013, http://www.sg-chem.net/.
19 J. Ouyang, X. Qianfei, C.-W. Chu, Y. Yanga, G. Li and J. Shinar, *Polymer*, 2004, **45**, 8443.
20 J. L. Bredas, F. Wudl and A. J. Heeger, *Solid State Commun.*, 1987, **63**, 577.
21 V. Rumbau, J. A. Pomposo, A. Eleta, J. Rodrigues, H. Grande, D. Mecerreyes and E. Ochoteco, *Biomacromolecules*, 2007, **8**, 315.

22 M. Yamashita, T. Sasaki, H. Okuzaki and C. Otani, *IEEE Xplore digital library*, DOI: 10.1109/IRMMW-THz.2012.6380295.
23 J. Ouyang, *ACS Appl. Mater. Interfaces*, 2013, **5**, 13082.
24 J. Casado, V. Hernandez, F. J. Ramirez and J. T. Lopez Navarrete, *J. Mol. Struct.: THEOCHEM*, 1999, **463**, 211.
25 S. S. Zade and M. Bendikov, *J. Phys. Chem. B*, 2006, **110**, 15839.
26 S. S. Zade and M. Bendikov, *Chem.–Eur. J.*, 2007, **13**, 3688.
27 C. Aleman and J. Casanovas, *J. Phys. Chem. A*, 2004, **108**, 1440.
28 G. Agalyaa, C. Lva, X. Wanga, M. Koyamaa, M. Kuboa and A. Miyamoto, *Surf. Sci.*, 2005, **244**, 195.
29 A. Dkhissi, D. Beljonne, R. Lazzaroni, F. Louwet and B. Groenendaal, *Theor. Chem. Acc.*, 2008, **119**, 305.
30 A. Dkhissi, D. Beljonnea and R. Lazzaronia, *Synth. Met.*, 2009, **159**, 546.
31 S. Nagarajan, J. Kumar, F. F. Bruno, L. A. Sammuelson and R. Nagarajan, *Macromolecules*, 2008, **41**, 3049–3052.